

叶片副翼摆角对两段式翼型气动性能的影响

祁良奎 柳建华 张 良 廖裕恺

(上海理工大学 能源与动力工程学院, 上海 200093)

摘 要:以 Spalart - Allmaras (S - A) 湍流模型为计算模型, 对风力机叶片 NACA0018 翼型在副翼摆角分别为 0° 、 5° 、 10° 和 15° 下的流体流动情况进行数值模拟, 分析不同攻角下带副翼翼型上升阻力性能曲线以及翼型表面压力分布云图和流场流线图, 研究不同摆角对带副翼翼型的空气动力学性能的影响。结果表明: 相同攻角时, 翼型的升力系数随着副翼摆角的增大而减小; 副翼摆角的增大可以增大翼型的失速攻角, 改善翼型周围流体的流动状况, 提高翼型周围特别是副翼周围流体流动稳定性, 抑制流动分离涡的形成。

关键词:副翼; 摆角; 失速; 涡

中图分类号: TK12 文献标识码: A

DOI: 10.16146/j.cnki.rndlgc.2016.09.008

引 言

风力机运行安全性和经济性要求必须降低叶片载荷从而有效降低发电成本, 传统的常规翼型已经不能满足风力机及其特殊运行环境的要求。尾缘襟翼被认为是风力机载荷控制方法中最具可行性的气动部件^[1]。NASA Lewis 研究中心最早把飞机上的尾缘襟翼引入到风力机^[2], 来改变翼型剖面形状, 提高升力。1979年, 风力机叶片变桨控制工具第一次采用副翼实际应用在 DOE/NASA 水平轴风力机^[3]。由于副翼可以改变翼型弯度, 有提升翼型阻力和升力特性, 改善其气动性能^[4], 因此国内外学者对副翼做了大量的研究工作。Adernsen P B 通过仿真研究表明尾缘襟翼在 5 MW 风力机上可降低疲劳载荷作用^[5], 每个叶片用 3 个尾缘襟翼可降低了 40% 的叶弯矩; 申正华等研究表明在大攻角和大升力下^[6], Gurney 副翼对水平轴风力机性能有显著影响。特别是副翼高度为 2% 的翼型弦长时, 可提高风力机功率 39% 以上; 韩中合等以风力机翼型 S809

为研究对象^[7], 设计分离式尾缘襟翼模型, 研究表明副翼与主体间的缝隙对翼型气动性能的影响很小, 但是尾缘襟翼提高了翼型的升力系数; 祖红亚等从副翼几何特性出发^[8], 分析了 0.4、0.3 和 0.2 的副翼相对长度对翼型气动性能的影响, 研究表明副翼相对长度 0.3% 和翼缝相对宽度 1.0% 时, 翼型的升力系数最大。上述研究工作表明副翼对翼型周围流场和翼型升、阻力特性有影响, 但是还有许多副翼的结构特性对翼型气动性能影响尚待研究。

本文以 NACA0018 翼型为研究对象, 采用数值模拟方法研究不同副翼摆动角度情况下, 翼型静态气动性能及其所对应的流场结构。

1 计算模型及验证

以经典翼型 NACA0018 为基础建立如图 1 所示的两段计算模型。其中 c 为翼型弦长, l 为主翼长度, w 为副翼长度, d 为翼缝宽度, θ 为副翼摆角, ($^\circ$)。本文取相对翼缝宽度 d/c 分别为 10‰、15‰和 20‰; 副翼摆角 θ 分别取 0° 、 5° 、 10° 和 15° 。

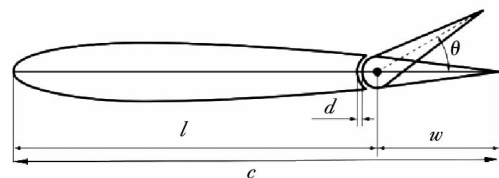


图 1 计算模型

Fig. 1 Computation model

图 2 是计算流域划分图, 其中边界条件 AGE、AB 和 ED 为速度入口, BD 为压力出口, AF 和 EF 为

收稿日期: 2015-11-10; 修订日期: 2016-01-11

基金项目: 上海市教育委员会重点学科资助项目 (J50502); 上海市科委建设项目 (13DZ2260900)

作者简介: 祁良奎 (1993-) 男, 河南信阳人, 上海理工大学硕士研究生。

流域交界面,翼型定义为无滑移壁面条件。为避免入口和出口边界的干扰,来流区域半径 $R_2 = 10c$,内部圆形区域半径 $R_1 = 1.2c$,尾流域边界 $AB = ED = 20c$ 。设定的空气参数为:密度 $\rho = 1.225 \text{ kg/m}^3$,动力黏度 $\mu = 1.7894 \times 10^{-5} \text{ kg/m} \cdot \text{s}$,来流风速 $v_\infty = 10 \text{ m/s}$,马赫数 $Ma = 0.03$,雷诺数 $Re = 6.85 \times 10^5$ (特征长度为翼型弦长)。计算流域划分的网格是在前半圆的来流区域采用二维结构网络,其它部分采用非结构网络,同时分别在翼型近壁面处进行局部网络加密和在内部圆形区域近壁面处采用边界层网络,保证了近壁面处复杂流动的计算精度。为了验证网格无关性,在比较多个不同网格数量的计算结果,确定计算区域网格总数 48 万,如图 3 所示。

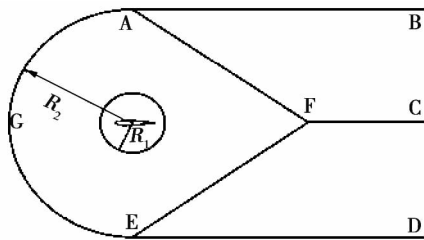


图 2 计算域划分

Fig.2 Division of the computation domain

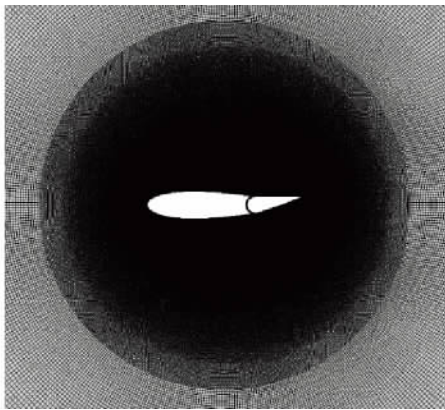


图 3 翼型周围网格划分

Fig.3 Mesh division around the airfoil

湍流模型采用 $S-A$ 模型,该模型控制方程相对简单,计算耗时短且容易收敛。它是通过求解输运方程得到湍流运动粘度的单方程湍流模型^[9],着重于恰当求解边界层受粘性影响的区域,在计算边界层受压力梯度限制的流动方面的结果非常好^[10]。

由于 Xfoil 有在计算失速前的翼型气动性能方

面精度高的特点^[11]因此本文将基准翼型的实验数据与 Xfoil 计算结果和 CFD 数值模拟结果比较验证,如图 4 所示。从图 4 可知,在翼型静态失速以前,Xfoil 和 CFD 的计算结果均与基准翼型的实验结果有较好吻合,但是在失速后,Xfoil 和 CFD 的计算结果与实验结果存在一定偏差但趋势一致,且在升力系数方面 CFD 计算结果更接近实验结果。因此从翼型升阻力特性上,本文采用的数值方法可靠。

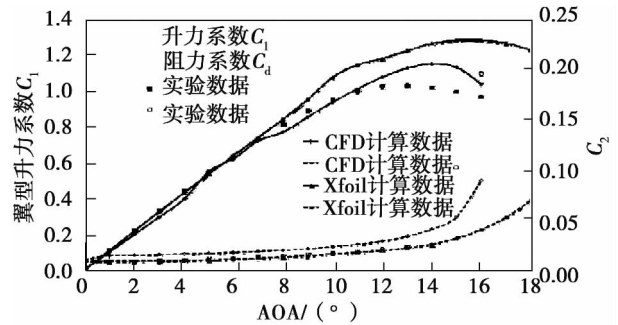


图 4 计算模型验证

Fig.4 Verification of the computation model

2 计算结果及分析

2.1 相对翼缝宽度对气动性能的影响

图 5 为相对翼缝宽度 d/c 分别为 10‰、15‰和 20‰时计算模型摆角在 0° 、 5° 、 10° 和 15° 时的升、阻力性能曲线。图中 C_l 为翼型升力系数, C_d 为翼型阻力系数, α 为攻角 0010、0015 和 0020 分别指 $d/c = 10‰$ 、 $15‰$ 和 $20‰$ 。

从图 5 可以看出,翼型的升力系数随着攻角的增大而不断增大,直至攻角达到失速攻角后迅速减小,翼型的升力系数随着摆角的增大而减小。从图 5(a)可以看出,副翼摆角为 0° 、 5° 、 10° 和 15° 时翼型的失速攻角均为 14° ,由此可以得出结论:在所研究范围内,当相对翼缝宽度 $d/c = 10‰$ 时,副翼摆角对翼型失速攻角的影响较小。观察图 5(b)可以发现,当 $d/c = 15‰$ 时,副翼摆角开始影响翼型的失速攻角;与图 5(a)相比 $\theta = 0^\circ$ 时翼型失速攻角为 14° ,而后 C_l 保持到攻角达到 16° 后迅速减小; $\theta = 5^\circ$ 时,翼型失速攻角为 16° , C_l 随攻角的增大略微减小,而对于 $\theta = 10^\circ$ 和 $\theta = 15^\circ$,二者的失速攻角均为 16° ,而 C_l 随攻角的继续增大立即减小。从图 5(c)可以看出 $d/c = 20‰$ 时, $\theta = 0^\circ$ 时翼型失速攻角为 14° , C_l

值随着攻角的继续增大直线减小; $\theta = 5^\circ$ 、 $\theta = 10^\circ$ 和 $\theta = 15^\circ$ 时翼型失速攻角已增大到 18° , 翼型已处于失速状态时。

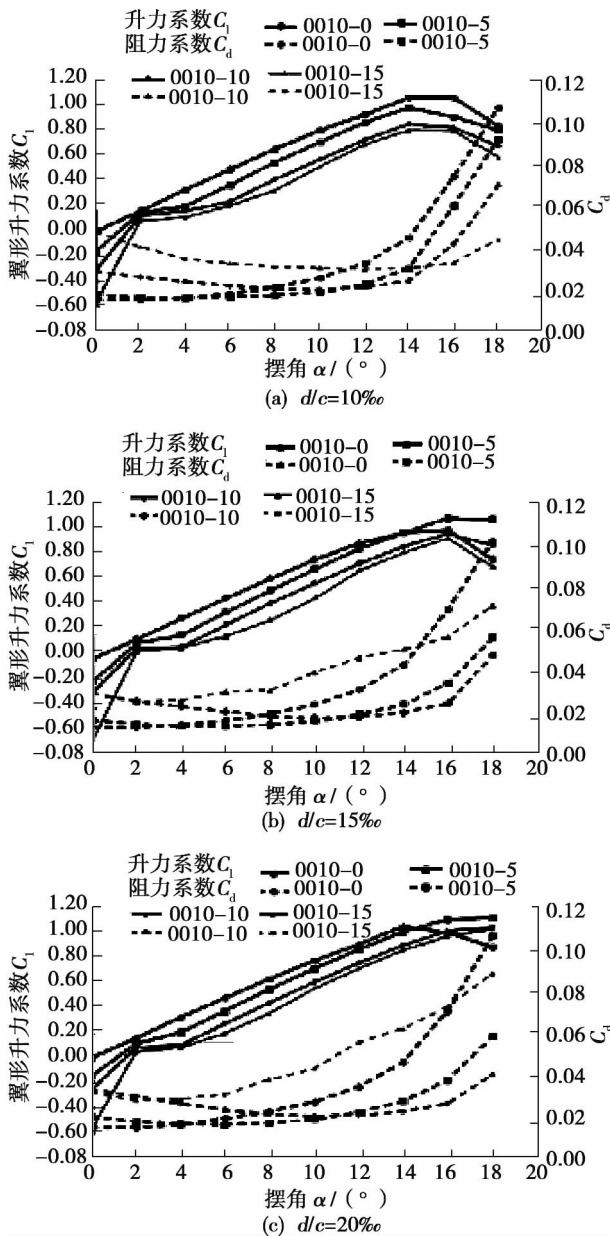


图 5 不同摆角翼型的升阻力系数曲线

Fig. 5 Lift drag coefficient curves of the airfoil at various swaying angles

图 6 是摆角分别为 0° 、 5° 、 10° 和 15° 时的翼型升阻比随攻角变化的曲线, 图中 K 为翼型的升阻比 $K = C_l/C_d$ 。从图中可以看出翼型升阻比随着攻角的增大先增大后减小, 升阻比存在一个最大值; 对比图 6 (a) ~ 图 6 (c) 可以发现, 相对翼缝宽度对翼型升阻比变化趋势影响较小, 最大升阻比对应的攻

角也基本不受相对翼缝宽度的影响。 $\theta = 0^\circ$ 时翼型达到最大升阻比对应的攻角为 8° , 而 $\theta = 5^\circ$ 、 $\theta = 10^\circ$ 和 $\theta = 15^\circ$ 时翼型最大升阻比对应的攻角则分别为 12° 、 14° 和 16° 。由此可以得出结论: 两段式翼型最大升阻比对应的攻角随着副翼摆角的增大而增大, 当 $d/c = 10\%$ 和 $d/c = 15\%$ 时, $\theta = 5^\circ$ 翼型的最大升阻比最大, $\theta = 10^\circ$ 次之, $\theta = 0^\circ$ 时最大升阻比小于 $\theta = 10^\circ$, $\theta = 15^\circ$ 时翼型的最大升阻比最小; 而当 $d/c = 20\%$, $\theta = 10^\circ$ 时翼型的最大升阻比还略大于 $\theta = 5^\circ$ 时翼型的最大升阻比。

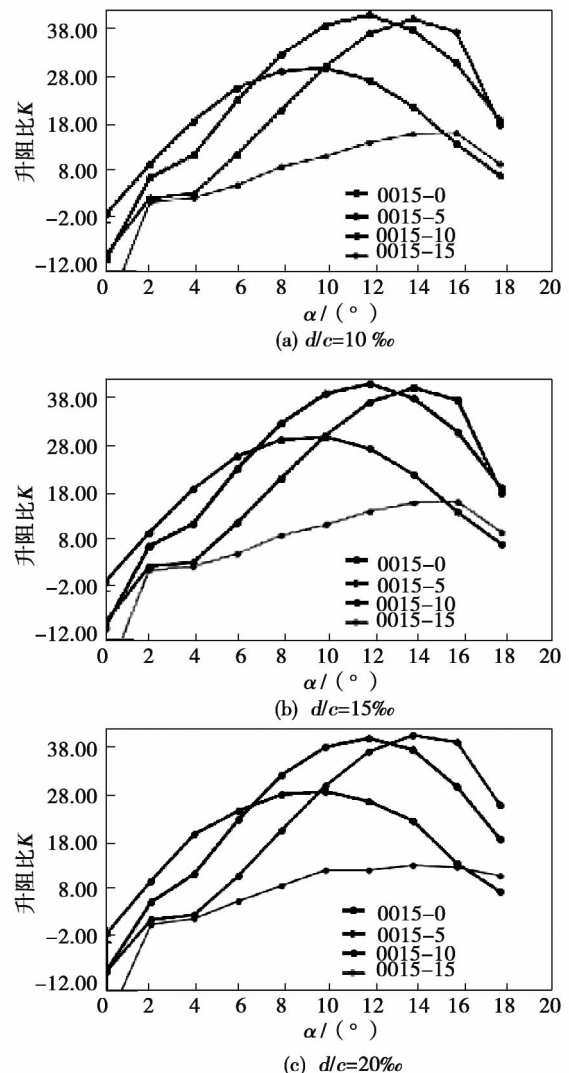


图 6 翼型的升阻比曲线

Fig. 6 Lift drag ratio curves of the airfoil

2.2 副翼摆角对气动性能的影响

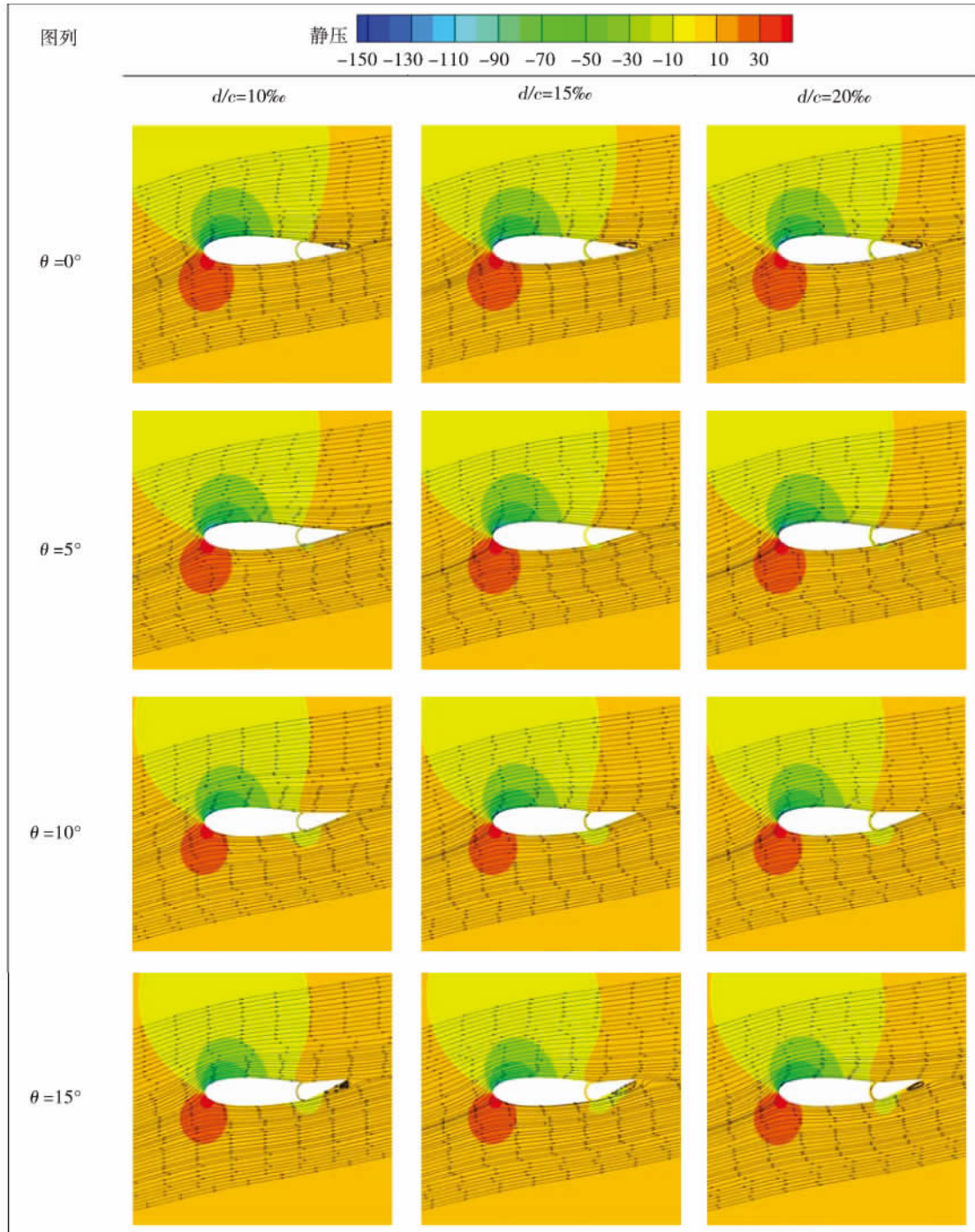
为进一步研究摆角影响副翼翼型气动性能的流体动力学机理, 从流体流动规律角度揭示上文现象

出现的原因 表 1 ~ 表 3 分别给出了 $\alpha = 12^\circ$ 、 $\alpha = 14^\circ$ 和 $\alpha = 16^\circ$ 时副翼摆角分别为 0° 、 5° 、 10° 和 15° 时

对应 $d/c = 10\%$ 、 15% 和 20% 下的翼型周围流体流动压力分布云图和流线图。

表 1 $\alpha = 12^\circ$ 翼型周围压力分布云图和流线图

Tab. 1 Contours of the distribution of the pressure around the airfoil when $\alpha = 12^\circ$ and streamline diagram



从表 1 中可以看出, 副翼摆角相同时, 较小攻角下相对翼缝宽度对翼型周围压力和流线分布影响较小。对于 $d/c = 10\%$, 当副翼摆角 $\theta = 0^\circ$ 时, 在副翼尾缘吸力面处出现分离涡, 此时涡的影响范围仅局

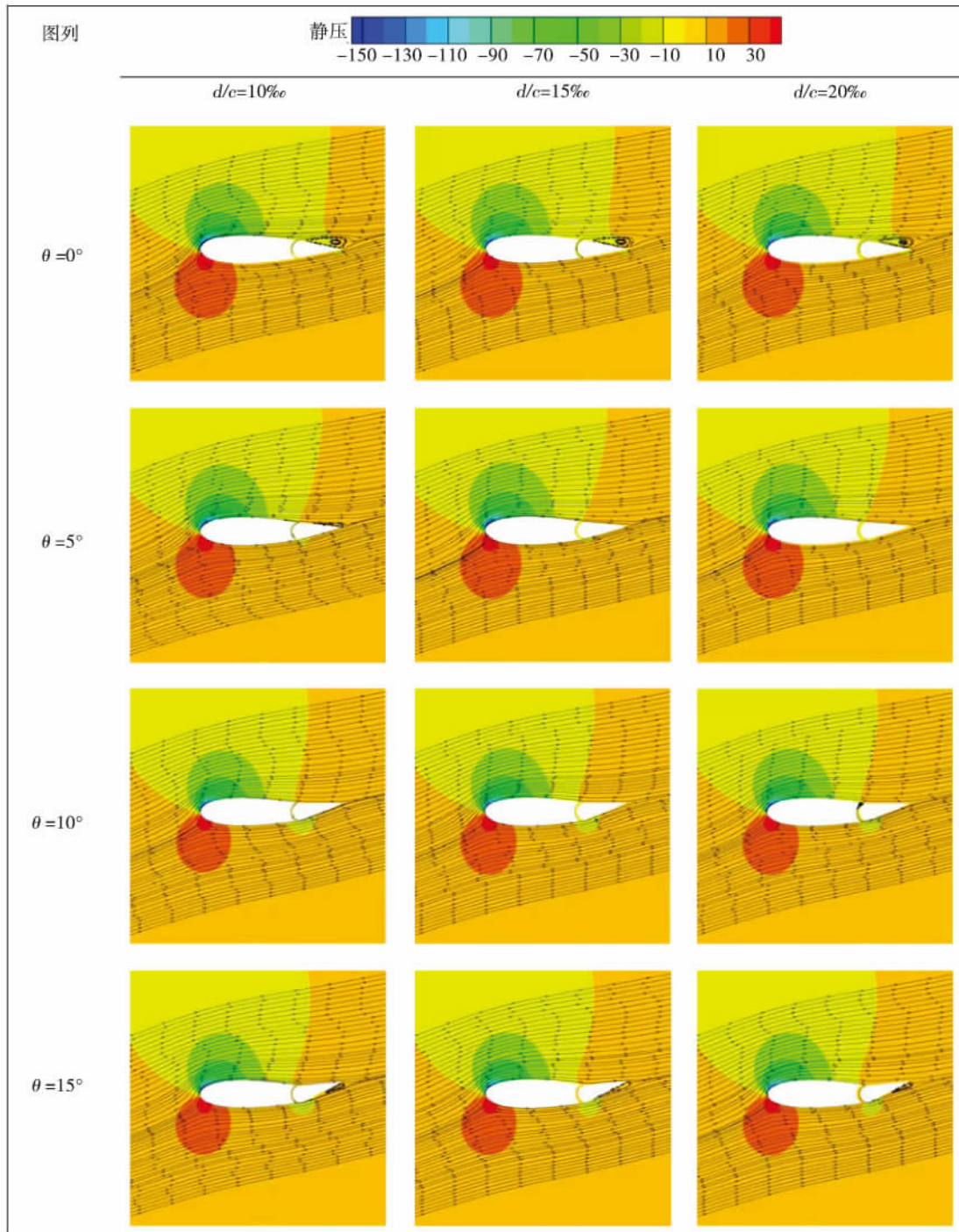
限于翼型尾缘处, 结构简单, 强度较弱; 摆角 $\theta = 5^\circ$ 时, 副翼尾缘处的分离涡消失, 仅在副翼开缝处压力面附近出现范围极小的低压区; 摆角 $\theta = 10^\circ$ 时, 副翼开缝处压力面附近低压区的范围较 $\theta = 5^\circ$ 时有所

扩大, 副翼上下表面均未出现分离涡; $\theta = 15^\circ$ 时, 在副翼尾缘压力面侧出现分离涡, 其影响范围仅局限于翼型尾缘处, 结构简单, 强度较弱, 副翼开缝处压

力面低压区的范围与 $\theta = 10^\circ$ 时相当。观察 $d/c = 15\%$ 和 $d/c = 20\%$ 可以得出相同的结论。

表 2 $\alpha = 14^\circ$ 翼型周围压力分布云图和流线图

Tab. 2 Contours of the distribution of the pressure around the airfoil and streamline diagram when $\alpha = 14^\circ$



从表 2 中可以看出, 副翼摆角相同时, 较大攻角下相对翼缝宽度对翼型周围压力和流线分布影响依然较小。当 $d/c = 10\%$ 、 $\theta = 0^\circ$ 时, 副翼吸力面侧出

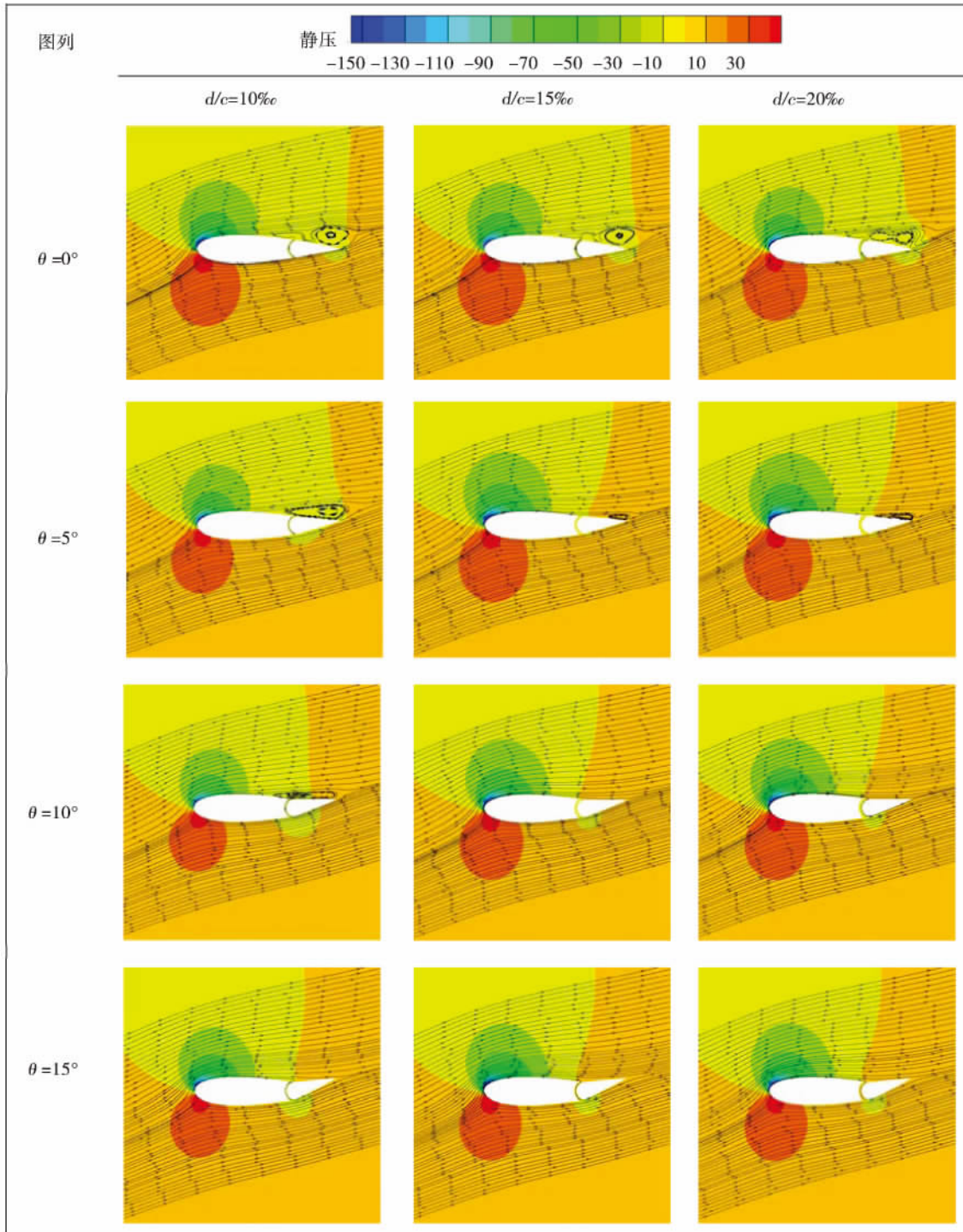
现分离涡, 其影响范围较 $\alpha = 12^\circ$ 时明显增大, 已完全覆盖副翼整个吸力面侧, 结构比较复杂; 摆角 θ 增大到 5° 时, 副翼吸力面侧分离涡的分布范围有所减

小,结构也较为简单,而此时 $d/c = 15\%$ 和 $d/c = 20\%$ 副翼上表面的分离涡消失,说明相对翼缝宽度可以起到提高翼型气动性能的作用; $\theta = 10^\circ$ 时,三种相对翼缝宽度的翼型副翼吸力面侧的分离涡均消

失,仅在副翼开缝处压力面侧出现范围较大的低压区; $\theta = 15^\circ$ 时,在副翼压力面侧出现分离涡,涡的影响范围局限在翼型尾缘处,涡的结构简单,对翼型尾缘后的流场无影响,副翼吸力面侧的分离涡消失。

表 3 $\alpha = 16^\circ$ 翼型周围压力分布云图和流线图

Tab. 3 Contours of the distribution of the pressure around the airfoil and streamline diagram when $\alpha = 16^\circ$



从表 3 中可以看出,大攻角时,摆角和相对翼缝宽度对翼型周围压力和流线分布均有较大的影响。

$d/c = 10\%$ 、 $\theta = 0^\circ$ 时,副翼吸力面侧的分离涡范围已延伸至 $1/2c$ 处,分离涡已对翼型后流场的结构产

生影响,进而对翼型的气动性能产生较大影响,翼型前缘点处高压区(图中红色区域)范围也比 $\alpha = 12^\circ$ 和 $\alpha = 14^\circ$ 时大; $\theta = 5^\circ$ 时,摆角的存在改善了空气扰流翼型的情况,减小了分离涡的范围,使其仅分布于副翼压力面侧,此时分离涡的范围还随着相对翼缝宽度的增大而减小; $\theta = 10^\circ$ 时,尾缘分离涡的范围进一步减小,已不再对翼型后缘流场结构产生影响, $d/c = 15\%$ 和 $d/c = 20\%$ 时副翼压力面侧的分离涡已完全消失;摆角 $\theta = 15^\circ$,不同相对翼缝宽度下副翼吸力面和压力面均未出现分离涡,翼型的气动性能明显得到改善。

3 结 论

通过对相对翼缝宽度为 10% 、 15% 和 20% 下副翼摆角分别为 0° 、 5° 、 10° 和 15° 时翼型周围流体流动状况进行数值模拟并对模拟结果进行后处理,在所研究范围内,可以得到如下结论:

(1) 翼型处于未失速状态时,相同攻角下,翼型升力系数随着副翼摆角的增大而减小;当攻角达到失速攻角后,相同攻角时翼型对应的升力系数则随着摆角的增大而增大,这说明了摆角在某种程度上可以改善翼型的空气动力学性能;

(2) 副翼摆角对翼型最大升阻比有较大影响,当 $d/c = 10\%$ 和 $d/c = 15\%$ 时, $\theta = 5^\circ$ 翼型的最大升阻比最大, $\theta = 10^\circ$ 次之, $\theta = 0^\circ$ 时最大升阻比小于 $\theta = 10^\circ$, $\theta = 15^\circ$ 时翼型的最大升阻比最小;而当 $d/c = 20\%$, $\theta = 10^\circ$ 时翼型的最大升阻比还略大于 $\theta = 5^\circ$ 时翼型的最大升阻比。相对翼缝宽度对翼型最大升阻比的影响较小;

(3) 副翼摆角的增大可以改善翼型周围流体的流动状况,提高翼型周围特别是副翼周围流体流动稳定性,抑制流动分离涡的形成。

参考文献:

[1] 李传峰. 风力机尾缘襟翼气动特性与机理研究[D]. 北京: 中国科学院工程热物理研究所, 2013.
LI Chuan-feng. Study of the aerodynamic characteristics and mechanism of the trailing edge flap in a wind turbine[D]. Beijing: Institute of Engineering Thermophysics, Chinese Academy of Sci-

ences, 2013.

- [2] Spera D A. Wind Turbine Technology: Fundamental Concepts of Wind Turbine Engineering[M]. New York: ASME Press, 2009.
- [3] 徐璋,王茜,皇甫凯林,等. 襟翼对垂直轴风力机性能影响的数值模拟[J]. 动力工程学报, 2011, 31(9): 715-719.
XU Zhang, WANG Qian, HUANGFU Kai-lin, et al. Numerical simulation of the influence of the flap on the aerodynamic performance of a vertical shaft wind turbine[J]. Journal of Power Engineering, 2011, 31(9): 715-719.
- [4] Chandrasekhara M S. Optimum Gurney flap height determination for "lost-lift" recovery in compressible dynamic stall control[J]. Aerospace Science and Technology, 2010, 14(8): 551-556.
- [5] Andersen P B. Advanced Load Alleviation for Wind Turbines Using Adaptive Trailing Edge Flaps: Sensing and Control[D]. Roskilde: Technical University of Denmark, 2010.
- [6] 申振华,于国亮. Gurney襟翼对水平轴风力机性能影响的实验研究[J]. 太阳能学报, 2007, 28(2): 196-199.
SHEN Zhen-hua, YU Guo-liang. Experimental investigation of the effect of the Gurney flap on the performance of a horizontal-shaft wind turbine[J]. Acta Energiae Solaris Sinica, 2007, 28(2): 196-199.
- [7] 韩中合,贾亚雷,李恒凡,等. 风力机分离式尾缘襟翼气动性能[J]. 农业工程学报, 2014, 30(20): 666-673.
HAN Zhong-he, JIA Ya-lei, LI Heng-fan, et al. Aerodynamic performance of the detachable type flap at the trailing edge in a wind turbine[J]. Transactions of Agricultural Engineering, 2014, 30(20): 58-64.
- [8] 祖红亚,李春,李润杰,等. 襟翼相对长度对翼型气动性能的影响[J]. 动力工程学报, 2015, 35(8): 58-64.
ZU Hong-ya, LI Chun, LI Run-jie, et al. Effect of the relative length of the flap on the aerodynamic performance of an airfoil[J]. Journal of Power Engineering, 2015, 35(8): 666-673.
- [9] 雷延生,周正贵. 风力机振荡翼型动态失速特性的CFD研究[J]. 太阳能学报, 2010, 31(3): 367-372.
LEI Yan-sheng, ZHOU Zheng-gui. CFD-based Investigation of the dynamic stall characteristics of the oscillating airfoil in a wind turbine[J]. Acta Energiae Solaris Sinica, 2010, 31(3): 367-372.
- [10] 廖书学,李春,聂佳斌,等. 不同翼型对垂直轴风力机性能的影响[J]. 机械设计与研究, 2011, 27(3): 108-111.
LIAO Shu-xue, LI Chun, NIE Jia-bin, et al. Influence of various airfoils on the performance of a vertical shaft wind turbine[J]. Machine Design and Research, 2011, 27(3): 108-111.
- [11] VERSTEEG H K, MALALASEKERA W. An introduction to computational fluid dynamics[M]. New York, USA: Wiley, 1995.

(刘瑶 编辑)

ing process of a water solution and pure water inside a vertical rectangular microchannel. Through comparison of the difference between the saturated flow and boiling heat exchange effectiveness and reliability of the water solution and pure water, the influence of the concentration on the heat exchange of the water solution was analyzed. It has been found that under the operating condition when $T_{in} = 368 \text{ K}$, $v = 0.5 \text{ m/s}$ and $q_w = 200 \text{ kW/m}^2$, the average value of the Nu number of the wall surface heated by the surfactant water solution along the flow direction in the saturated boiling stage will be higher than that of pure water. When $t = 60 \text{ ms}$, in the zone closing to the outlet of the flow passage, both wall surfaces heated by the water solution and pure water will be locally overheated but the highest overheated temperature corresponding to the water solution will be higher than that corresponding to pure water and the overheated surface areas will be relatively small. In a range from 0.256 mol/L to 0.769 mol/L , to increase the concentration of the water solution will enhance the saturated flow and boiling heat exchange effectiveness and the heat exchange of water solution at a concentration of 0.513 mol/L will be reliable. **Key words:** microchannel, surfactant water solution, flow boiling, saturated boiling, numerical simulation

管式换热器黏液形成菌生物污垢特性的实验研究 = **Experimental Study of the Bio-foul Characteristics of Bacteria Formed in Viscous Liquids Inside a Tubular Type Heat Exchanger** [刊, 汉] / XU Zhi-ming, WANG Yu-hang, SHEN Yi-wen, WANG Jing-tao (College of Energy Source and Power Engineering, Northeast University of Electric Power, Jilin, China, Post Code: 132012) // Journal of Engineering for Thermal Energy & Power. - 2016, 31 (9). - 39 ~ 44

To exploratorily investigate the foul characteristics of bacteria formed in viscous liquids inside a tubular type heat exchanger, with the bacteria formed in viscous liquids obtained from the slime at the bottom of the circulating cooling towers in a power plant after the separation and purification serving as the object of study, a foul dynamic simulation and test system was utilized and a contrast test research method was adopted to obtain the foul characteristics of bacteria formed in viscous liquids in a stainless steel bare tube heat exchanger under the condition of various inlet temperatures, flow speeds and volumetric concentrations. It has been found that there exists an induction period in the fouling process of bacteria formed in viscous liquids. With an increase of the temperature at the inlet, the induction period will become shortened and the time duration required by the foul thermal resistance to attain its asymptotic value reduced. In the range of the temperature tested, when the temperature at the inlet is $30 \text{ }^\circ\text{C}$, the asymptotic value of the foul thermal resistance will be maximum followed by the asymptotic value at $35 \text{ }^\circ\text{C}$ and minimum at $25 \text{ }^\circ\text{C}$. With an increase of the flow speed, the time duration required by the foul thermal resistance to attain its asymptotic value will become shortened and the asymptotic value of the foul thermal resistance will decrease. With an increase of the volumetric concentration, the induction period will become prolonged, the fouling speed rate will increase and the asymptotic value of the foul thermal resistance will become big. **Key words:** tubular type heat exchanger, foul characteristics, bacteria formed in viscous liquids, bio-film, enzyme

叶片副翼摆角对两段式翼型气动性能的影响 = **Influence of the Swaying Angle of the Flap of a Blade on the**

Aerodynamic Performance of a Dual-section Type Airfoil [刊 汉]/QI Liang-kui ,LIU Jian-hua ,ZHANG Liang ,LIAO Yu-kai (College of Energy Source and Power Engineering ,Shanghai University of Science and Technology ,Shanghai ,China ,Post Code: 200093) ,LIU Jian-hua (Shanghai City Key Laboratory on Multi-phase Flow and Heat Transfer in Power Engineering ,Shanghai ,China ,Post Code: 200093) //Journal of Engineering for Thermal Energy & Power. -2016 31(9) . -45 ~ 51

With the Spalart-Allmaras(S-A) turbulent flow model serving as the calculation model ,a numerical simulation of the fluid flow conditions of the NACA0018 airfoil was performed under the condition of the swaying angle of the flap being 0 degree ,5 degrees ,10 degrees and 15 degrees respectively. In this connection ,the lifting drag performance curves of the airfoil provided with a flap ,contours of the distribution of the pressure on the surface of the airfoil and the flow field streamline chart at various attack angles were also analyzed and the influence of the swaying angle on the aerodynamic performance of the airfoil provided with a flap was studied. It has been found that at a same attack angle ,the lifting force coefficient of the airfoil will decrease with an increase of the swaying angle of the flap. To increase the swaying angle of the flap can increase the attack angle of the airfoil when it goes into a stall ,improve the flow conditions of the fluid around the airfoil ,enhance the flow stability of the fluid around the airfoil ,especially around the flap and contain the formation of the flow-separation-caused vortexes. **Key words:** flap ,swaying angle ,stall ,vortex

基于气动弹性剪裁的风力机叶片模态分析 = Analysis of the Modal of a Blade in a Wind Turbine Based on the Aeroelastic Tailoring [刊 汉]/CHEN Wen-pu ,LI Chun ,YE Zhou ,MIAO Wei-pao (College of Energy Source and Power Engineering ,Shanghai University of Science and Technology ,Shanghai ,China ,Post Code: 200093) ,LI Chun ,YE Zhou (Shanghai City Key Laboratory on Multi-phase Flow and Heat Transfer in Power Engineering ,Shanghai ,China ,Post Code: 200093) //Journal of Engineering for Thermal Energy & Power. -2016 31(9) . -52 ~ 57

To study the influence of the lamination parameters of a blade on its dynamic characteristics ,prevent the blade from any resonance and improve the characteristics of the blade in mechanics ,established was a finite element model for blades in a 1.5 MW wind turbine. Through changing the angle and the fiber proportion of the lamination layer ,the authors implemented a variety of the lamination layers of the blade in various ply plate structure and conducted an analysis of the modal of various lamination structures of the blade above mentioned ,obtained the first six order intrinsic frequencies and vibration patterns of various models and analyzed the causes of the lamination parameters influencing the dynamic characteristics of the blade. It has been found that the composite materials have their significant anisotropy and to change the angle of the lamination layer can influence the magnitude of the intrinsic frequency. The flapwise and edgewise vibration will dominate the low order vibration patterns of the blade and to increase the proportion of the lamination layers at an angle of 0 degree can enhance the low order intrinsic frequency and the torsional vibration will occur in the high order modal. The lamination layer at an angle of 45 degrees can enhance the torsion-resistant capacity of the blade and contribute to enhancing the high order intrinsic frequency. **Key**